Harvesting entanglement from the cylindrical gravitational wave spacetime*

Feifan He (何非凡)[1] Yongjie Pan (潘永杰)[1] Baocheng Zhang (张保成)[1†]

[1]School of Mathematics and Physics, China University of Geosciences, Wuhan 430074, China

Abstract: We investigate the entanglement harvesting protocol within the context of cylindrical gravitational waves given first by Einstein and Rosen, focusing on the interactions between non-relativistic quantum systems and linearized quantum gravity. We study how two spatially separated detectors can extract entanglement from the specific spacetime in the presence of gravitational waves, which provides a precise quantification of the entanglement that can be harvested using these detectors. In particular, we obtain the relation between harvested entanglement and the distance to wave sources that emits gravitational waves and analyze the detectability using quantum Fisher information. The enhanced detectability demonstrates the advantages of cylindrical symmetric gravitational waves.

Keywords: gravitational wave, cylindrical symmetry, quantum field effect, entanglement harvesting

DOI: **CSTR:**

I. INTRODUCTION

Entanglement harvesting [1, 2], refers to the process by which detectors independently coupled to a quantum field can become entangled by extracting entanglement from the field. This mechanism operates within a multipartite quantum system framework, comprising the combined Hilbert spaces of the detectors and the field. Typically modeled using a scalar field, this setup facilitates the transfer of virtual particles between detectors, thereby inducing entanglement among them. The possibility of entanglement harvesting from spacelike separated regions is unique to quantum fields, as classical fields do not possess entanglement that can be extracted. This distinction has been utilized to determine the quantum or classical nature of a field. Notably, it has been proposed that employing an entanglement harvesting protocol with the gravitational field could serve as a direct witness to quantum gravity [3, 4]. This approach underscores the pivotal role of quantum field properties in facilitating such quantum phenomena.

Initially explored in flat spacetime scenarios [1, 2], this phenomenon of entanglement harvesting has been extensively investigated under various conditions, including cosmological backgrounds [5, 6], noninertial frames [7, 8], black hole environments [9, 10], and in the presence of gravitational waves (GWs) [11, 12]. Further studies have considered entanglement harvesting when detectors interact with distinct field operators [13−15] and when placed in superpositions of different temporal orders or trajectories [16, 17].

The entanglement harvested by two Unruh-DeWitt (UDW) detectors [18, 19] is highly sensitive to the frequency of the gravitational wave. This can reveal the "information content" about gravitational-wave memory effect and supertranslations [11, 12]. Other investigations into entanglement harvesting from the vacuum including gravitational waves involved the quantum degrees of freedom of gravity by coupling GWs to a scalar quantum field [20−22]. In these studies, the GWs were considered as planar waves, which could manifest that the vacuum in the presence of GWs are quantum, but cannot reveal any other information about the wave sources. In this paper, we will investigate entanglement harvesting in the context of cylindrical GWs of Einstein and Rosen (called also Einstein-Rosen waves, or ERWs) [23−26] and discuss the information about the distance from the wave sources obtained through the analyses on the entanglement change between two UDW detectors.

The ERW, an exact solution to general relativity characterized by two commuting Killing vectors, aptly describes a cylindrical GW. Historically, the ERW was pivotal in early explorations to quantify the energy transported by GWs [28−31], a challenging task due to the local non-descriptiveness of GW energy caused by the equivalence principle [32, 33], which showed that the observation of ERWs is feasible. Moreover, the quantum aspects of the ERWs have been rigorously formulated [34], and its quantization in conjunction with a massless scalar field has been successfully achieved [35]. This facilitates

Received 10 February 2025; Accepted 14 April 2025

* This work is supported by National Natural Science Foundation of China (NSFC) with Grant No. 12375057 and the Fundamental Research Funds for the Central Universities, China University of Geosciences (Wuhan)

† E-mail: zhangbaocheng@cug.edu.cn

the study about entanglement harvesting from the ERW spacetime. In particular, the ERWs carry the information about the distance from the wave sources, which might be transferred to the harvested entanglement between the detectors, as will be investigated in this paper.

This paper is organized as follows. In Section II, the protocol of entanglement harvesting is revisited using two spacelike separated detectors that are accelerating in the flat spacetime. In Section III, the quantized formalism of the weak cylindrical GWs, and how the detectors are coupled to the GWs are described. Meanwhile, entanglement harvesting from the spacetime in the presence of linear cylindrical GWs is studied and the information about the distance from the wave sources is revealed in this section. The conclusions is given in Section IV.

II. ENTANGLEMENT HARVESTING PROTOCOL

A. The Untuh-DeWitt detector

We consider two identical UDW detectors, labeled A and B. Each detector is a two-level system with a ground state $|g\rangle_D$ and an excited state $|e\rangle_D$, where $D\in\{A,B\}$. The energy difference between these states is denoted by Ω_D. These detectors interact locally with a massless quantum scalar field, represented as $\hat{\phi}(x,t)$. The path followed by each detector through spacetime is specified by $x_D(\tau_D)$, where τ_D is the proper time experienced by the detector D. The interaction between each detector and the scalar field is governed by a Hamiltonian specific to each detector,

$$H_D(\tau)=\lambda_D\chi_D(\tau)\left(f_D^*(x)e^{i\Omega_D\tau}\sigma_D^+ + f_D(x)e^{-i\Omega_D\tau}\sigma_D^-\right)\phi(x), \quad (1)$$

where $\lambda_D\ll 1$ represents a small coupling strength of each detector to the scalar field. The switching function, $\chi_D(\tau)$, regulates the timing of the interaction, turning the coupling to the field on and off. $f_D(x)$ is the smearing function which controls the spatial region of the interaction. The ladder operators, which facilitate transitions between the detector states, are defined as $\sigma_D^+=|e\rangle_D\langle g|_D$ and $\sigma_D^-=|g\rangle_D\langle e|_D$. These operators are crucial in our quantum mechanical model, which effectively describes light-matter interactions without involving angular momentum exchange.

The time evolution of the detector-field system is governed by the unitary operator $\hat{U}$, defined as

$$\hat{U}=\mathcal{T}\exp\left[-\int dt\left(\frac{d\tau_A}{dt}\hat{H}_A[\tau_A(t)]+\frac{d\tau_B}{dt}\hat{H}_B[\tau_B(t)]\right)\right] \quad (2)$$

where $\mathcal{T}$ is the time-ordering operator that arranges the operators from earliest to latest times as we move from right to left in the exponential.

Initially, both detectors A and B start in their ground states, and the field is in its vacuum state. The combined initial state of the system is

$$|\varphi_0\rangle=|g\rangle_A\otimes|g\rangle_B\otimes|0\rangle_\phi. \quad (3)$$

After the interaction, the state of the detectors is described by a density matrix $\hat{\rho}_{AB}=Tr_\phi\left[\hat{U}|\varphi_0\rangle\langle\varphi_0|\hat{U}^\dagger\right]$, obtained by tracing out the field states from the total system state. This results in

$$\hat{\rho}_{AB}=\begin{pmatrix} 1-\mathcal{L}_{AA}-\mathcal{L}_{BB} & 0 & 0 & \mathcal{M}^* \\ 0 & \mathcal{L}_{BB} & \mathcal{L}_{BA} & 0 \\ 0 & \mathcal{L}_{AB} & \mathcal{L}_{AA} & 0 \\ \mathcal{M} & 0 & 0 & 0 \end{pmatrix}+O(\lambda^2) \quad (4)$$

to lowest order in the coupling strength. The density matrix (4) is expressed in the basis $\{|g_Ag_B\rangle,|g_Ae_B\rangle,|e_Ag_B\rangle,|e_Ae_B\rangle\}$. Here $\mathcal{L}_{AA}$ and $\mathcal{L}_{BB}$ represents the probability of detector being excited, and $\mathcal{L}_{AB}$, $\mathcal{L}_{BA}$, and $\mathcal{M}$ measures the coherence between the detectors due to their interaction with the field, reflecting nonlocal effects between the two detectors at different times. Their expressions are given as

$$\mathcal{L}_{IJ}=\lambda_I\lambda_J\int d\tau_I d\tau_J\chi_I(\tau_I)\chi_J(\tau_J)f_I(x_I)f_J^*(x_J) \times e^{-(\Omega_I\tau_J-\Omega_I\tau_J)}W(x_I(t),x_J(t')) \quad (5)$$

and

$$\mathcal{M}=\lambda_A\lambda_B\int d\tau_A d\tau_B\chi_A(\tau_A)\chi_B(\tau_B)f_A(x_A)f_B^*(x_B) \times e^{-(\Omega_A\tau_A+\Omega_B\tau_B)}\theta(t'-t) \times(W(x_A(t),x_B(t'))+W(x_B(t),x_A(t'))) \quad (6)$$

where $\theta(t-t')$ is the Heaviside function. The Wightman function $W(x,x')=\langle 0|\hat{\phi}(x(t),t),\hat{\phi}(x'(t'),t')|0\rangle$ is a fundamental field correlator that quantifies the vacuum fluctuations of the field between two spacetime points $x(t)$ and $x'(t')$, crucial for understanding the field's influence on the detectors.

When we consider only one of the detectors, either A or B, by tracing out the other one from the combined density matrix (Eq. 4), we arrive at a simplified description for the state of the remaining detector,

$$\hat{\rho}_D=\begin{pmatrix} 1-\mathcal{L}_C & 0 \\ 0 & \mathcal{L}_C \end{pmatrix}. \quad (7)$$

In this matrix, $\mathcal{L}_C$ represents the probability that the detector A or B transitions from its ground state to its excited state due to its interaction with the field.

B. Negativity

To explore the entanglement between two identical UDW detectors after local interactions with a quantum field, we use a measure called negativity [36, 37]. Negativity is a reliable quantifier for entanglement between two qubits, suitable for situations such as entanglement harvesting as discussed in previous studies. The negativity of a system, $\mathcal{N}$, is determined by summing the negative eigenvalues from the partial transpose of the density matrix $\hat{\rho}_D$,

$$\mathcal{N} = \max\left(0, \sqrt{|\mathcal{M}|^2 - \frac{(\mathcal{L}_{AA}-\mathcal{L}_{BB})^2}{4}} - \frac{\mathcal{L}_{AA}+\mathcal{L}_{BB}}{2}\right). \quad (8)$$

In cases where the detectors have equal excitation probabilities, $\mathcal{L}_{AA} = \mathcal{L}_{BB} = \mathcal{L}$, the formula simplifies to

$$\mathcal{N} = \max(0, |\mathcal{M}| - \mathcal{L}). \quad (9)$$

Assuming both detectors are identical with equal interaction strengths, frequencies, and simultaneous interactions in their respective frames, we can use the following expressions to compute the necessary probabilities and correlation terms from the Fourier transforms of the switching functions,

$$\mathcal{L}_{IJ} = \frac{\lambda^2}{(2\pi)^3}\int \frac{d^3\mathbf{k}}{2|\mathbf{k}|}\tilde{\chi}^*(\Omega+|\mathbf{k}|)\tilde{\chi}(\Omega+|\mathbf{k}|)\tilde{f}_I(\mathbf{k})\tilde{f}_J^*(\mathbf{k}), \quad (10)$$

$$\mathcal{M} = -\frac{\lambda^2}{(2\pi)^3}\int \frac{d^3\mathbf{k}}{2|\mathbf{k}|}Q(|\mathbf{k}|,\Omega)(\tilde{f}_A(-\mathbf{k})\tilde{f}_B(\mathbf{k})+\tilde{f}_B(-\mathbf{k})\tilde{f}_A(\mathbf{k})), \quad (11)$$

where

$$Q(|\mathbf{k}|,\Omega) = \int dt dt' \chi(t)\chi(t') e^{i(\Omega+|\mathbf{k}|)t'} e^{i(\Omega-|\mathbf{k}|)t}\theta(t-t'), \quad (12)$$

and we have defined the Fourier transform of $f(\mathbf{x}) = \psi_e(\mathbf{x})\psi_g^*(\mathbf{x})$ and $\chi(t)$ as

$$\tilde{f}(\mathbf{k}) = \int d^3\mathbf{x}\, f(\mathbf{x}) e^{i\mathbf{k}\cdot\mathbf{x}}, \quad (13)$$

$$\tilde{\chi}(\omega) = \int dt\, \chi(t) e^{i\omega t}. \quad (14)$$

It is noted that the results are obtained using the assumption that $\lambda_A = \lambda_B = \lambda$, $\Omega_A = \Omega_B = \Omega$, $\chi_A(t) = \chi_B(t) = \chi(t)$, and the smearings are identical modulo a spatial translation. In the later calculations in this paper, this assumption will be maintained.

The concept of entanglement harvesting using two UDW detectors linearly coupled to a scalar quantum field has been investigated in the literature [8, 9, 11, 14, 17, 38−41]. But in the curved spacetime, what information about the curved spacetime can be obtained from the harvested entanglement was hardly investigated. This is the task of this paper, and in what follows we will investigate how to extract the information about the distance from the wave sources by the harvested entanglement from the vacuum of the cylindrical GW spacetime.

III. EINSTEIN-ROSEN WAVES

In this section we study the situation in which two UDW detectors are coupled to the cylindrical GWs. We are going to implement the entanglement harvesting protocol and analyze the information about the distance from the wave sources using Fisher information.

A. Quantized Cylindrical Gravitational Waves

Since the observable effect of cylindrical GWs is considered at the place with a large distance from the source, the linearized metric is adequate for our purpose with the form as

$$ds^2 = (1-\psi)ds_3^2 + (1+\psi)dZ^2, \quad (15)$$

where $ds_3^2 = -(1+\gamma)dT_C^2 + (1+\gamma)dR^2 + R^2 d\theta^2$, and ψ and γ are functions of only R and T_C. It derives from the spacetime metric of ERWs [23, 34, 42, 43], $ds^2 = e^{\gamma-\psi}(-dT_C^2 + dR^2) + e^{-\psi}R^2 d\theta^2 + e^{\psi}dZ^2$, in which ψ encodes the physical degrees of freedom and satisfies the usual wave equation for an axially symmetric massless scalar field in three-dimensions,

$$\partial_{T_C}^2\psi - \partial_R^2\psi - \frac{1}{R}\partial_R\psi = 0. \quad (16)$$

The metric function γ can be expressed as [44], $\gamma(R) = \frac{1}{2}\int_0^R d\bar{R}\bar{R}\left[(\partial_{T_C}\psi)^2 + (\partial_{\bar{R}}\psi)^2\right]$, and $\gamma_\infty = \frac{1}{2}\int_0^\infty dR R \left[(\partial_{T_C}\psi)^2 + (\partial_R\psi)^2\right]$, where $\gamma(R)$ and γ_∞ are the energy of the scalar field in a ball of radius R and in the whole two-dimensional flat space, respectively.

When the regularity at the origin $R=0$ is imposed [44], the solutions for the field ψ can be expanded in the form

$$\psi(R,T_C)=\int_0^\infty\frac{d\mathbf{k}}{\sqrt{2}}J_0(R\mathbf{k})\left[A(\mathbf{k})e^{-ikT_C}+A^\dagger(\mathbf{k})e^{ikT_C}\right],\quad(17)$$

where $A(\mathbf{k})$ and $A^\dagger(\mathbf{k})$ are fixed by the initial conditions and are complex conjugate to each other, because ψ and J_0 (the zeroth-order Bessel function of the first kind) are real. In principle, the quantization of the field ψ can be carried out in a standard way. We can introduce a Fock space in which $\hat{\psi}(R,0)$, the quantum counterpart of $\psi(R,0)$, is an operator-valued distribution [45]. Its action is determined by the usual annihilation and creation operators, $\hat{A}(\mathbf{k})$ and $\hat{A}^\dagger(\mathbf{k})$, whose only non-vanishing commutators are $\left[\hat{A}(\mathbf{k}_1),\hat{A}^\dagger(\mathbf{k}_2)\right]=\delta(\mathbf{k}_1,\mathbf{k}_2)$.

The Hamiltonian of this linearized gravity can be written as [34, 42, 46],

$$H_0=\int_0^R dR\left(\frac{p_{\hat{\psi}}^2}{2R}+\frac{R}{2}\left(\frac{\partial\hat{\psi}}{\partial R}\right)\right),\quad(18)$$

where the gauge fixing conditions $p_\gamma=0$ and $R=r$. $p_{\hat{\psi}}$ and p_γ are the canonical momenta conjugated to the metric fields $\hat{\psi}$ and γ, respectively. $R=r$ indicates that R can be used to measure the distance from the source to the detector. It is not hard to confirm that $H_0=\gamma_\infty=\int_0^\infty d\mathbf{k}\,\mathbf{k}\hat{A}^\dagger(\mathbf{k})\hat{A}(\mathbf{k})$ when the expression of $p_{\hat{\psi}}$ is used.

To get a unit asymptotic timelike Killing vector field in the actual four-dimensional spacetime [47, 48], one must transfer the time coordinate by $T_C=e^{-\gamma_\infty/2}t$. In this asymptotic region $R\to\infty$, ∂_t is a unit timelike vector. t is the physical time, and the corresponding physical Hamiltonian is given as [42, 47, 48], $H=E(H_0)=2(1-e^{-H_0/2})$. Thus, the annihilation operator with respect to the physical time can be linked to $\hat{A}(\mathbf{k})$ by $\hat{A}_E(\mathbf{k},t)=\hat{A}(\mathbf{k})\exp[-itE(\mathbf{k})e^{-H_0/2}]$. In the first approximation, the physical field $\hat{\psi}=\int_0^\infty\frac{d\mathbf{k}}{\sqrt{2}}J_0(R\mathbf{k})\left[\hat{A}_E(\mathbf{k},t)+\hat{A}_E^\dagger(\mathbf{k},t)\right]$ has the similar time-evolved form to Eq. (17). When the UDW detectors are coupled to the linearized cylindrical GWs, the physical Hamiltonian H should be considered, but in the first-order perturbation, $H\simeq H_0$ and $t\simeq T_C$. Thus, the results in the coordinates (T_C,R,θ,Z) can be used in the actual interaction between the detectors and the linearized cylindrical GWs, as seen in the next section.

B. Entanglement Harvesting

We start with the interaction Hamiltonian between gravitational waves and two free falling detectors [15]

$$\hat{H}_I(t)=\lambda\mathcal{R}_{0i0j}(t,\hat{\mathbf{x}})\hat{x}^i\hat{x}^j,\quad(19)$$

where $\lambda=\sqrt{\frac{\pi}{2}}\frac{m}{m_p}$, with m_p being the Planck mass. Here, λ serves as a dimensionless coupling constant, essentially scaling with the detector's rest mass measured in Planck units. This formulation allows us to quantitatively assess the gravitational effects on quantum mechanical scales. There are some other ways (see the discussions in Ref. [15]) to describe the interaction between the detectors and an external weak gravitational field, while we choose the same way as in Ref. [15] which could be obtained by considering a wave function in curved spacetimes, since for our study the quantum states for the detectors and the quantum description for ERWs are explicit as presented in the following calculations.

Assuming that the energy levels of our detector's free Hamiltonian are discrete, we can expand the interaction Hamiltonian in terms of the system's wavefunctions as

$$\begin{aligned}\hat{H}_I(t)&=\lambda\chi(t)\int d^3\mathbf{x}\mathcal{R}_{0i0j}(t,\mathbf{x})x^ix^j|\mathbf{x}\rangle\langle\mathbf{x}|_t\\&=\lambda\chi(t)\sum_{nm}\int d^3\mathbf{x}\mathcal{R}_{0i0j}(t,\mathbf{x})x^ix^jf_{nm}^*(\mathbf{x})e^{i\Omega_{nm}t}|n\rangle\langle m|,\quad(20)\end{aligned}$$

where $f_{nm}(\mathbf{x})=\psi_n(\mathbf{x})\psi_m^*(\mathbf{x})$ is the smearing function, $|\mathbf{x}\rangle\langle\mathbf{x}|_t$ denotes the position operator in the interaction picture, and the switching function is added here in order to ensure the finite interaction time. The functions $\psi_n(\mathbf{x})=\langle\mathbf{x}|n\rangle$ represent the wavefunctions corresponding to the energy eigenvalues E_n, and $\Omega_{nm}=E_n-E_m$ represents the energy difference between states. In our calculation, the detectors are regarded as two-level atoms, such as the ground state and an excited state, and the respective wavefunctions are $\psi_g(\mathbf{x})=\langle\mathbf{x}|g\rangle$ for the ground state and $\psi_e(\mathbf{x})=\langle\mathbf{x}|e\rangle$ for the excited state. This simplified model allows us to focus on the key dynamical aspects of the quantum system under the influence of an external gravitational field. Then, the interaction Hamiltonian can be written as

$$\begin{aligned}\hat{H}_I(t)=\lambda\chi(t)\int d^3\mathbf{x}(F^{ij*}(\mathbf{x})e^{i\Omega t}\hat{\sigma}^++F^{ij}(\mathbf{x})e^{-i\Omega t}\hat{\sigma}^-)\\\times\mathcal{R}_{0i0j}(t,\mathbf{x}),\quad(21)\end{aligned}$$

where the energy difference between the excited state $|e\rangle$ and the ground state $|g\rangle$ is denoted by $\Omega=\Omega_{eg}=E_e-E_g$. The function $F^{ij}(\mathbf{x})=\psi_e(\mathbf{x})\psi_g^*(\mathbf{x})x^ix^j$ represents the smearing tensors, which are crucial for modeling the interaction of the detector with the linearized gravitational field. The ladder operators are defined as $\hat{\sigma}^+=|e\rangle\langle g|$, and $\hat{\sigma}^-=|g\rangle\langle e|$. Additionally, the terms in the Hamiltonian that commute with the detector's free Hamiltonian have been neglected, as they do not contribute to the entanglement dynamics but only shift the energy levels. For the quantization, it can be implemented by replacing the curvature tensor $\mathcal{R}_{0i0j}(t,\mathbf{x})$ with the operator-valued distribution $\hat{\mathcal{R}}_{0i0j}(x)$ in the Hamiltonian. This model provides a framework for understanding the interaction between a localized quantum system and a weak quantum gravitational field.

To leading order in λ, the excitation probability of the detector after the interaction can be expressed as

$$\mathcal{L}^G = \lambda^2 \int d^4x d^4x' \chi(t)\chi(t') F^{ij}(\mathbf{x}) F^{kl*}(\mathbf{x}') e^{-i\Omega(t-t')} \times \langle \hat{\mathcal{R}}_{0i0j}(x) \hat{\mathcal{R}}_{0k0l}(x') \rangle_0. \tag{22}$$

This equation shows how the excitation probability can be transformed into a single momentum integral based on the curvature two-point function. This formulation is crucial for quantitatively describing how quantum systems respond to gravitational fields, offering insights into their probabilistic behavior under such influences. The curvature fluctuation which is given by $R_{0R0R}(R,T) = -\frac{1}{2}\partial_T^2 h_{RR}$ ($h_{RR} = \psi(R,T)$ as seen in Eq. (15)) can be obtained as

$$\hat{\mathcal{R}}_{0R0R}(R,T) = \int \frac{d\mathbf{k}}{2\sqrt{2}} |\mathbf{k}|^2 J_0(\mathbf{k}R) \times \left[\hat{A}(\mathbf{k}) e^{-ikT} + \hat{A}^{\dagger}(\mathbf{k}) e^{ikT}\right], \tag{23}$$

where Eq. (17) is used. Then, the curvature two-point function is calculated as

$$\left\langle \hat{\mathcal{R}}_{0R0R}(R) \hat{\mathcal{R}}_{0R0R}(R') \right\rangle_0 = \int \frac{d\mathbf{k}}{8} |\mathbf{k}|^4 J_0(\mathbf{k}R) J_0(\mathbf{k}R') e^{-ik(T-T')}. \tag{24}$$

Thus,

$$\mathcal{L}^G = \lambda^2 \frac{4T^2\sigma^8}{15\pi} \int d|\boldsymbol{k}| \, |\boldsymbol{k}|^{10} J_0(\boldsymbol{k}R) J_0(\boldsymbol{k}(R-L)) \times e^{-|\boldsymbol{k}|^2\sigma^2} e^{-T^2(|\boldsymbol{k}|+\Omega)^2}. \tag{25}$$

where in the calculation the switching functions are taken as $\chi_A(t) = \chi_B(t) = \chi(t) = \frac{1}{\sqrt{2\pi}} \exp(-t^2/2T^2)$, and the smearing functions are takens as $f_A(x) = \frac{1}{(2\pi\sigma^2)^{3/2}} \exp(-x^2/2\sigma^2)$, $f_B(x) = \frac{1}{(2\pi\sigma^2)^{3/2}} \exp(-(x-L)^2/2\sigma^2)$ where T represents a duration timescale, σ determines the spatial width of the smearing function, and L is the separation between the detectors.

Similarly, given the choices of gaps and spacetime smearing functions, the resulting expression for the nonlocal term $\mathcal{M}^G$ can be obtained as

$$\mathcal{M}^G = -\lambda^2 \frac{4T^2\sigma^8}{L^5\pi} \int d|\mathbf{k}| \, |\mathbf{k}|^5 J_0(\mathbf{k}R) J_0(\mathbf{k}(R-L)) e^{-|\mathbf{k}|^2\sigma^2} \times e^{-T^2(|\mathbf{k}|^2+\Omega^2)} (1 - \mathrm{erf}[i|\mathbf{k}|T)(3|\mathbf{k}|L\cos(|\mathbf{k}|L) + (|\mathbf{k}|^2L^2 - 3)\sin(|\mathbf{k}|L)]. \tag{26}$$

In Figs. 1, 2 and 3, we present the numerical results for the negativity.

In Fig. 1, we plot the negativity of the two-detector system as a function of the detectors' energy gap, for different values of the separation between them. We see that there is a minimum threshold on the required energy gap before any entanglement is acquired between the detectors. Once the threshold energy gap is met, there is a rapid increase in the negativity, until it peaks. This is a similar behavior to entanglement harvesting from a real scalar field, where the detectors gap can be tuned to maximize the harvested entanglement (see, [41]).

In Fig 2, we plot the entanglement acquired by the detectors as a function of their energy gaps for varying detector sizes. We conclude that as the detectors increase in size, the harvested entanglement increases. This can be traced back to the fact that the interaction of the detectors with the gravitational field is proportional to their sizes squared.

In Fig. 3, we plot the negativity of the detectors state as a function of σ for a fixed ΩT and varying values of L. We clearly see a monotonic increase in the negativity with σ. We also see the result that the negativity decreases only after the ratio σ/T exceeds about 0.57 as the separation between the detectors increases.

In Fig. 4, we present how the entanglement harvested by detectors varies with the distance from the source of gravitational waves, taking into account different distances between the detectors themselves. We find that the harvested entanglement diminishes as the source distance increases, a phenomenon linked to the weakening strength of gravitational waves as they propagate from

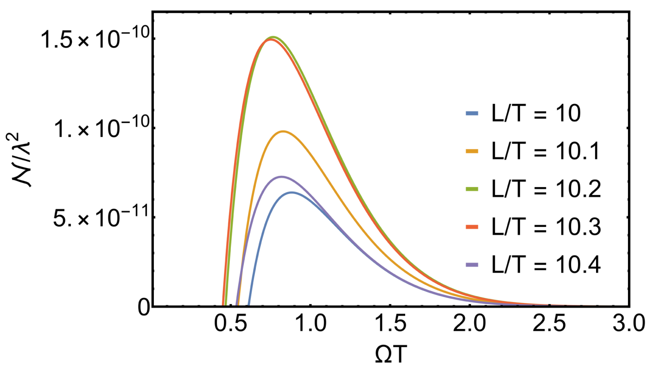

Fig. 1. (color online) Negativity as a function of the detectors' gap Ω for multiple values of the detectors separation distance L. We fixed the detectors size to be $\sigma = 0.3T$ for each of the plots. Other parameter is taken as $R/T = 1000$.

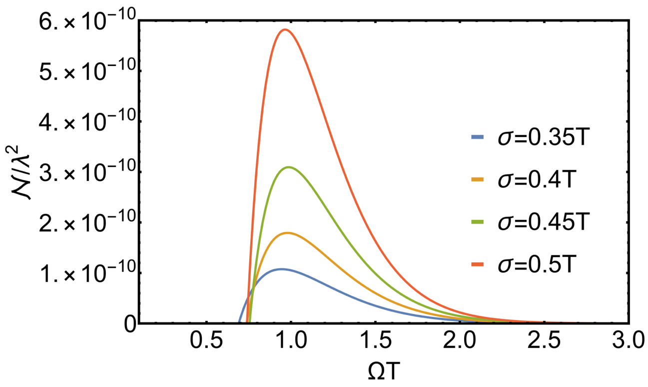

Fig. 2. (color online) Negativity as a function of the detectors' gap Ω for multiple values of the detectors' size σ. We fixed the separation between the detectors to be $L=10T$ for each of the plots. Other parameters is taken as $R/T=1000$.

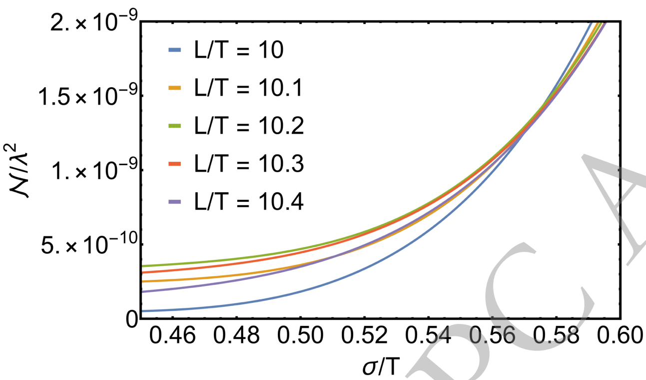

Fig. 3. (color online) Negativity as a function of the detectors size σ for multiple values of the detectors separation L. We fixed the energy gap of the detectors as $\Omega T=0.77$ for each of the plots. Other parameter is taken as $R/T=1000$.

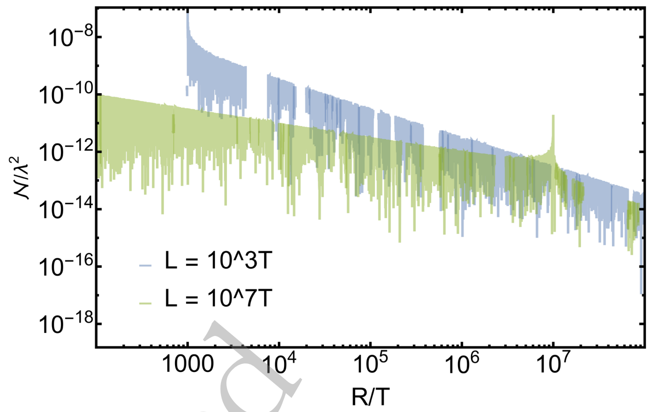

Fig. 4. (color online) Negativity as a function of gravitational waves source distance R for multiple values of the detectors separation L. We fixed the energy gap of the detectors as $\Omega T=0.77$ for each of the plots. Other parameters is taken as $\sigma/T=1000$.

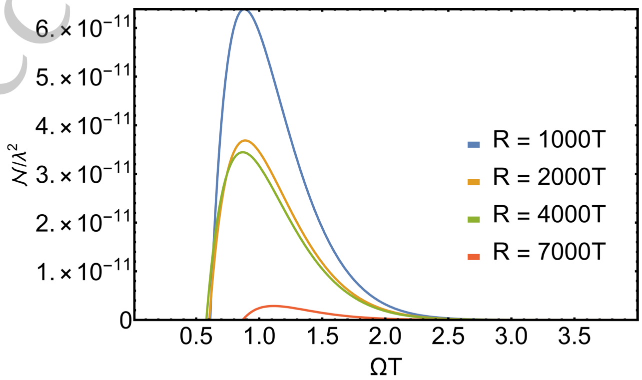

Fig. 5. (color online) Negativity as a function of energy gap for multiple values of the source distance R. We fixed the detector separation $L=10T$ as for each of the plots. Other parameters is taken as $\sigma/T=1000$.

their origin.

Additionally, in Fig. 5, we explore the relationship between the entanglement harvested by the detectors and their energy gap across various source distances. The analysis confirms that as the distance from the source increases, the entanglement decreases, underscoring the impact of gravitational wave attenuation over distance.

Finally we comment on realistic scales for the entanglement that can be harvested by a physical system interacting with the cylindrical gravitational field. Our plots for the negativity yielded (at best) $\mathcal{N}^G\sim\lambda^2 5*10^{-7}$. Recall that the dimensionless coupling constant λ is given by $\sqrt{\frac{\pi}{2}}m/m_p$. If the mass of the system is of the order of the mass of a hydrogen atom we would have $\lambda^2\sim10^{-38}$, so that the harvested negativity gives $\mathcal{N}^G\sim10^{-46}$. This result demonstrates that the entanglement harvested using cylindrical symmetry is significantly greater than that observed in entanglement harvesting from the gravitational field using hydrogen-like atoms at a source distance of $R=1000T$, as reported in [15]. Furthermore, even at a much larger distance of $R=9\times10^7T$, the harvested entanglement, $\mathcal{N}^G\approx10^{-55}$, still exceeds previous findings by 16 orders of magnitude. These findings show the enhanced capability of detectors with cylindrical symmetry to harvest entanglement from the GW field.

C. Quantum Fisher Information

In order to understand the information about the distance from the sources, carried by the cylindrical GWs, we apply the concept of quantum Fisher information (QFI) to investigate the possibility of measurement.

According to the quantum Cramér-Rao theorem [49, 50], for a given observable source distance R, the measurement precision is determined by

$$Var(R)\geq\frac{1}{n\mathcal{F}_Q(R)}, \tag{27}$$

where Var is the covariant variance, and n represents the number of repeated measurements. $\mathcal{F}_Q$ is the QFI defined by [51]

$$\mathcal{F}_Q(R)=\frac{\left(\partial_R(1-\dot{\mathcal{L}}^G)\right)^2}{\dot{\mathcal{L}}^G}+\frac{\left(\partial_R\dot{\mathcal{L}}^G\right)^2}{\dot{\mathcal{L}}^G}=2\frac{\left(\partial_R\dot{\mathcal{L}}^G\right)^2}{\dot{\mathcal{L}}^G},\tag{28}$$

then we have the transition rate as

$$\begin{aligned}\dot{\mathcal{L}}^G=&\lambda^2\frac{8T\sigma^8}{15\pi}\int d|\boldsymbol{k}||\boldsymbol{k}|^{10}J_0(\boldsymbol{k}R)J_0(\boldsymbol{k}(R-L))\\&\times e^{-|\boldsymbol{k}|^2\sigma^2}e^{-T^2(|\boldsymbol{k}|+\Omega)^2}\\&-\lambda^2\frac{8T^3\sigma^8}{15\pi}\int d|\boldsymbol{k}||\boldsymbol{k}|^{10}\\&\times J_0(\boldsymbol{k}R)J_0(\boldsymbol{k}(R-L))e^{-|\boldsymbol{k}|^2\sigma^2}\\&\times(|\boldsymbol{k}|+\Omega)^2e^{-T^2(|\boldsymbol{k}|+\Omega)^2}\\=&\lambda^2\frac{8T\sigma^8}{15\pi}\int d|\boldsymbol{k}||\boldsymbol{k}|^{10}\\&\times J_0(\boldsymbol{k}R)J_0(\boldsymbol{k}(R-L))e^{-|\boldsymbol{k}|^2\sigma^2}\\&\times e^{-T^2(|\boldsymbol{k}|+\Omega)^2}\left[1-T^2(|\boldsymbol{k}|+\Omega)^2\right].\end{aligned}\tag{29}$$

and

$$\begin{aligned}\partial_R\dot{\mathcal{L}}^G=&\lambda^2\frac{8T\sigma^8}{15\pi}\int d|\boldsymbol{k}||\boldsymbol{k}|^{11}[-J_1(\boldsymbol{k}R)J_0(\boldsymbol{k}(R-L))\\&-J_0(\boldsymbol{k}R)J_1(\boldsymbol{k}(R-L))]e^{-|\boldsymbol{k}|^2\sigma^2}e^{-T^2(|\boldsymbol{k}|+\Omega)^2}\\&\times\left[1-T^2(|\boldsymbol{k}|+\Omega)^2\right].\end{aligned}\tag{30}$$

Finally, we obtained the expression for the QFI as

$$\begin{aligned}\mathcal{F}_Q(R)=&2\lambda^2\frac{8T\sigma^8}{15\pi}\int d|\boldsymbol{k}||\boldsymbol{k}|^{11}(-J_1(\boldsymbol{k}R)J_0(\boldsymbol{k}(R-L))\\&-J_0(\boldsymbol{k}R)J_1(\boldsymbol{k}(R-L)))\\&\times e^{-|\boldsymbol{k}|^2\sigma^2}e^{-T^2(||\boldsymbol{k}|+\Omega)^2}\left(1-T^2(|\boldsymbol{k}|+\Omega)^2\right)\end{aligned}\tag{31}$$

The measurement uncertainty is defined by

$$U_R=\frac{\sigma_R}{R},\tag{32}$$

where $\sigma_R=\sqrt{Var(R)}$. We found that, for our model, when the wave source distance satisfies $R/L<200$, the uncertainty in measuring the wave source distance is approximately 21%. Moreover, the QFI decreases rapidly as R increases as shown in Fig. 6. This level of uncertainty is comparable to LIGO's measurements of binary neutron star merger events (10%-20%) and is lower than the uncertainty in measurements of binary black hole merger events (20%-50%) [52, 53]. Moreover, it is noted that Fig. 6 exhibits abrupt, non-smooth behavior, which is derived from the oscillatory Bessel functions. These functions, combined with the exponential suppression term, introduce a resonance effect that leads to abrupt changes in the QFI.

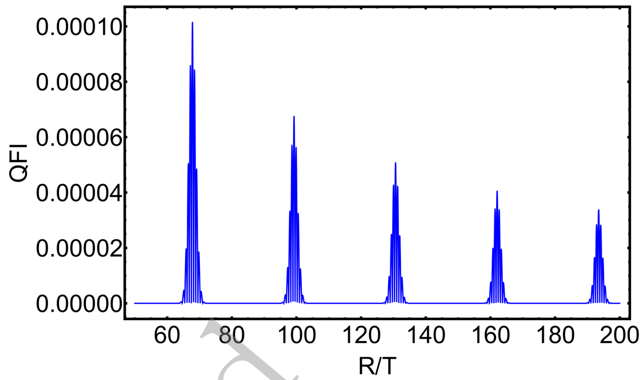

Fig. 6. (color online) The plot displays the absolute value of the QFI as a function of the normalized wave source distance. The parameters used are $\sigma=0.3T$, $\Omega T=0.1$, and $L=10T$.

IV. CONCLUSION

In this paper, we have explored the entanglement harvesting protocol within the spacetime in the presence of cylindrical gravitational waves, revealing results that markedly contrast with those from scenarios involving standard quantum gravitational field. The magnitude of entanglement negativity is substantially greater than that harvested from the vacuum of a conventional gravitational field. Importantly, our research elucidates the relationship between entanglement harvesting and the source distance of gravitational waves.

This significant discrepancy highlights the unique quantum structure and entanglement properties of the vacuum state associated with cylindrical GWs. It indicates that these specialized gravitational configurations may be particularly effective for entanglement harvesting, potentially enabling the observation of the information about the distance from sources at scales much larger than previously thought possible.

References

[1] A. Valentini, Phys. Lett. A **153**, 321 (1991)

[2] B. Reznik, Foundations of Physics **33**, 167 (2003)

[3] R. Faure, T. R. Perche, and B. d. S. L. Torres, Phys. Rev. D **101**, 125018 (2020)

[4] J. P. M. Pitelli and T. R. Perche, Phys. Rev. D **104**, 065016 (2021)
[5] G. Ver Steeg and N. C. Menicucci, Phys. Rev. D **79**, 044027 (2009)
[6] E. Martin-Martinez and N. C. Menicucci, Class. Quantum Grav. **29**, 224003 (2012)
[7] G. Salton, R. B. Mann, and N. C. Menicucci, New J. Phys. **17**, 035001 (2015)
[8] Z. Liu, J. Zhang, R. B. Mann, and H. Yu, Phys. Rev. D **105**, 085012 (2022)
[9] E. Tjoa and R. B. Mann, JHEP **2020**, 155 (2020)
[10] K. Gallock-Yoshimura, E. Tjoa, and R. B. Mann, Phys. Rev. D **104**, 025001 (2021)
[11] Q. Xu, S. A. Ahmad, and A. R. Smith, Phys. Rev. D **102**, 065019 (2020)
[12] F. Gray, D. Kubizňák, T. May, S. Timmerman, and E. Tjoa, JHEP **2021**, 1 (2021)
[13] A. Sachs, R. B. Mann, and E. Martín-Martínez, Phys. Rev. D **96**, 085012 (2017)
[14] T. R. Perche, C. Lima, and E. Martín-Martínez, Phys. Rev. D **105**, 065016 (2022)
[15] T. R. Perche, B. Ragula, and E. Martín-Martínez, Phys. Rev. D **108**, 085025 (2023)
[16] L. J. Henderson, A. Belenchia, E. Castro-Ruiz, C. Budroni, M. Zych, Č. Brukner, and R. B. Mann, Phys. Rev. Lett. **125**, 131602 (2020)
[17] J. Foo, R. B. Mann, and M. Zych, Phys. Rev. D **103**, 065013 (2021)
[18] W. G. Unruh, Phys. Rev. D **14**, 870 (1976)
[19] B. S. DeWitt, *Quantum gravity: the new synthesis*, in *General Relativity: An Einstein centenary survey*, edited by S. W. Hawking and W. Israel, (Cambridge University Press, 1979), pp. 680–745.
[20] M. Cliche and A. Kempf, Phys. Rev. D **83**, 045019 (2011)
[21] B.-H. Chen and D.-W. Chiou, Phys. Rev. D **105**, 024053 (2022)
[22] T. Prokopec, Class. Quantum Grav. **40**, 035007 (2023)
[23] A. Einstein and N. Rosen, Journal of the Franklin Institute **223**, 43 (1937)
[24] J. Weber and J. A. Wheeler, Rev. Mod. Phys. **29**, 509 (1957)
[25] D. Bini, A. Geralico, and W. Plastino, Class. Quantum Grav. **36**, 095012 (2019)
[26] F. He and B. Zhang, Phys. Rev. D **105**, 106019 (2022)
[27] L. C. B. Crispino, A. Higuchi, and G. E. A. Matsas, Rev. Mod. Phys. **80**, 787 (2008)
[28] K. S. Thorne, Phys. Rev. **138**, B251 (1965)
[29] S. Chandrasekhar, Proceedings of the Royal Society of London. A. Mathematical and Physical Sciences **408**, 209 (1986)
[30] T. Mishima and S. Tomizawa, Phys. Rev. D **96**, 024023 (2017)
[31] K. A. Bronnikov, N. Santos, and A. Wang, Class. Quantum Grav. **37**, 113002 (2020)
[32] R. A. Isaacson, Phys. Rev. **166**, 1263 (1968)
[33] V. F. Mukhanov, L. R. W. Abramo, and R. H. Brandenberger, Phys. Rev. Lett. **78**, 1624 (1997)
[34] K. Kuchař, Phys. Rev. D **4**, 955 (1971)
[35] J. Fernando Barbero G., I. Garay, and E. J. S. Villaseñor, Phys. Rev. Lett. **95**, 051301 (2005)
[36] G. Vidal and R. F.Werner, Phys. Rev. A **65**, 032314 (2002)
[37] M. B. Plenio, Phys. Rev. Lett. **95**, 090503 (2005)
[38] A. Pozas-Kerstjens, J. Louko, and E. Martín-Martínez, Phys. Rev. D **95**, 105009 (2017)
[39] L. J. Henderson, R. A. Hennigar, R. B. Mann, A. R. H. Smith, and J. Zhang, Class. Quantum Grav. **35**, 21LT02 (2018)
[40] N. Stritzelberger, L. J. Henderson, V. Baccetti, N. C. Menicucci, and A. Kempf, Phys. Rev. D **103**, 016007 (2021)
[41] H. Maeso-García, T. R. Perche, and E. Martín-Martínez, Phys. Rev. D **106**, 045014 (2022)
[42] J. D. Romano and C. G. Torre, Phys. Rev. D **53**, 5634 (1996)
[43] J. Celestino, H. de Oliveira, and E. Rodrigues, Phys. Rev. D **93**, 104018 (2016)
[44] A. Ashtekar and M. Pierri, J. Math. Phys. **37**, 6250 (1996)
[45] M. Reed and B. Simon, *Methods of Modern Mathematical Physics: Fourier Analysis, Self-Adjointness* (Academic Press, New York, USA, 1975).
[46] J. Fernando Barbero G., G. A. Mena Marugán, and E. J. S. Villaseñor, Phys. Rev. D **67**, 124006 (2003)
[47] A. Ashtekar and M. Varadarajan, Phys. Rev. D **50**, 4944 (1994)
[48] M. Varadarajan, Phys. Rev. D **52**, 2020 (1995)
[49] S. L. Braunstein and C. M. Caves, Phys. Rev. Lett. **72**, 3439 (1994)
[50] S. L. Braunstein, C. M. Caves, and G. J. Milburn, Ann. Phys. **247**, 135 (1996)
[51] M. G. Paris, International Journal of Quantum Information **7**, 125 (2009)
[52] B. P. Abbott, R. Abbott, T. Abbott, *et al.*, Phys. Rev. Lett. **119**, 161101 (2017)
[53] S. Nissanke, D. E. Holz, S. A. Hughes, N. Dalal, and J. L. Sievers, The Astrophysical Journal **725**, 496 (2010)